

000 001 002 003 004 005 006 007 008 009 010 011 012 013 014 015 016 017 018 019 020 021 022 023 024 025 026 027 028 029 030 031 032 033 034 035 036 037 038 039 040 041 042 043 044 045 046 047 048 049 050 051 052 053 GENERALIZED PREF-SHAP TO EXPLAIN PREFERENCE FUNCTIONS

Anonymous authors

Paper under double-blind review

ABSTRACT

We address the problem of feature attribution for skew-symmetric preference functions in dueling data settings, using the cooperative game-theoretic concept of *Shapley values*. Building on Pref-SHAP[Hu et al. (2022)], we propose *Generalized Pref-SHAP*, a framework that extends its applicability to a broader class of preference functions. Our method leverages a simple neural network to model arbitrary feature mappings while exploiting the canonical block structure inherent to skew-symmetric functions, enabling more meaningful explanations. Additionally, we explore foundational questions about Pref-SHAP, including its relationship with the block decomposition structure of skew-symmetric generalized preference function (GPM)[Hu et al. (2022)]. We perform experiments on a range of synthetic datasets to demonstrate the effectiveness and efficiency of our approach.

1 INTRODUCTION

Pairwise preference learning, often modeled via *dueling data*, plays a central role in ranking, recommender systems, sports tournaments, voting, online games etc. A common framework for modeling such pairwise data involves *skew-symmetric preference functions*, i.e., the function $f(u, v)$ satisfies $f(u, v) = -f(v, u)$, representing the preference for item u over item v , where $u, v \in \mathbb{R}^d$. We can represent such functions using the following *canonical form*[Rajkumar et al. (2021), Veerathu & Rajkumar (2021)]:

$$f(u, v) = u^\top A v, \quad (1)$$

where, d is even and $A \in \mathbb{R}^{d \times d}$ is a block-diagonal matrix composed of $d/2$ skew-symmetric 2×2 rotation matrices $\begin{bmatrix} 0 & -1 \\ 1 & 0 \end{bmatrix}$. This bilinear structure naturally arises in modeling utilities and comparisons, and is particularly amenable to analysis due to its algebraic simplicity and geometric structure. While modeling preference functions has received considerable attention[Negahban et al. (2015), Rajkumar & Agarwal (2016), Chen & Joachims (2016), Makhijani & Ugander (2019), Bower & Balzano (2020)], explaining their predictions, that is, attributing the model’s output to individual input features, remains less explored. Recent work, notably Pref-SHAP[Hu et al. (2022)], extends the classical Shapley value[Shapley et al. (1953)] to the setting of pairwise comparisons, assigning feature-level attributions to preference decisions using a game-theoretic lens. We aim to investigate both the theoretical and practical behaviors of Pref-SHAP in non-parametric model setting based on the canonical form.

1.1 MAIN CONTRIBUTIONS

- **Block Structure Consistency:** We analyze whether Pref-SHAP respects the block structure inherent in the canonical form. This reveals how well the Shapley attributions align with the inherent feature pairing in the model.
- **Theoretical Analysis Under Canonical Form:** We derive closed-form expressions for Pref-SHAP values when $f(u, v) = u^\top A v$, focusing on the two-feature case for clarity. We explore how the attributions are affected by distributional properties like feature variance, constancy, and independence. Our analysis identifies unintuitive behaviors that arise from interaction effects and the symmetry axiom in Shapley values, and suggests that interaction-aware explanations may be necessary in some cases.

054
 055
 056
 057
 058
 059
 060
 061
 062
 063
 064
 065
 066
 067
 068
 069
 070
 071
 072
 073
 074
 075
 076
 077
 078
 079
 080
 081
 082
 083
 084
 085
 086
 087
 088
 089
 090
 091
 092
 093
 094
 095
 096
 097
 098
 099
 100
 101
 102
 103
 104
 105
 106
 107

- **Generalization to Arbitrary Feature Mappings[2]:** We extend Pref-SHAP to work with nonlinear or learned feature maps ϕ , proposing *Generalized Pref-SHAP*. This new framework preserves the interpretability of Shapley decompositions while leveraging the structure in A , enabling explanations in complex models with deep representations.

2 BACKGROUND MATERIALS

2.1 PREFERENCE LEARNING

We consider a more general class of skew-symmetric functions of the form:

$$f(u, v) = \langle \phi(u), A\phi(v) \rangle, \quad (2)$$

where $u, v \in \mathbb{R}^k$, $\phi : \mathbb{R}^k \rightarrow \mathbb{R}^d$ is a feature mapping(possibly nonlinear) with even d , and $A \in \mathbb{R}^{d \times d}$. Any skew-symmetric function can be represented in this form, where ϕ is the identity function and $k = d$. The likelihood function used for such models, especially in pairwise preference scenarios, often takes the form:

$$p(y | u, v) = \sigma(y \cdot f(u, v)) = 1 - p(y | v, u), \quad (3)$$

where $\sigma(x) = \frac{1}{1+e^{-x}}$ is the sigmoid function and $y \in \{-1, 1\}$ indicates the preference label.

2.2 SHAPLEY VALUE

The purpose of this paper is to study the local explainability of predictions based on preference functions using the *Shapley value*[Shapley et al. (1953)], a concept from cooperative game theory. It is basically a credit allocation method where a subset of k players is assigned a value function based on their contribution to a game $\nu : [0, 1]^k \rightarrow \mathbb{R}$. The Shapley value for player j in game ν is given by:

$$\Phi_j(\nu) = \sum_{S \subseteq \Omega \setminus \{j\}} \frac{|S|!(d - |S| - 1)!}{d!} [\nu(S \cup \{j\}) - \nu(S)],$$

where, $\Omega = \{1, \dots, d\}$ is the set of d players.

It satisfies several desirable uniqueness axioms such as efficiency(6), symmetry, null player property, linearity. The use of this concept in explainable ranking context helps in finding feature attribution in a model prediction by creating a correspondence between the concept of players and item features. In particular, linearity ensures that for a linear ensemble of models, the Shapley value of a feature is the corresponding linear combination of individual model Shapley values.

2.3 PREF-SHAP

In the Pref-SHAP framework[Hu et al. (2022)], the value function is adapted to model the pairwise preference setting.

2.4 PREFERENTIAL VALUE FUNCTION FOR ITEMS[HU ET AL. (2022); CHAU ET AL. (2022B),GRÜNEWÄLDER ET AL. (2012)]

Definition 1. Given a preference function $f \in \mathcal{H}$, and a pair of items $(x^l, x^r) \in \mathcal{X} \times \mathcal{X}, \mathcal{X} \subseteq \mathcal{R}^d$, the preferential value function $\nu : \mathcal{X} \times \mathcal{X} \times [0, 1]^k \times \mathcal{H} \rightarrow \mathbb{R}$ for computing Shapley values (Φ) in Pref-SHAP is defined as the following conditional expectation:

$$\nu_{x^l, x^r, S}(f) = \mathbb{E}_r \left[f(\{X_S^l, X_{S^c}^l\}, \{X_S^r, X_{S^c}^r\}) \mid X_S^l = x_S^l, X_S^r = x_S^r \right], \quad (4)$$

where $S \subseteq \{1, \dots, k\}$ is a subset of feature indices, and X is the input random vector. The notation X_S denotes the subvector of features indexed by S , and S^c is the complement of S . The pair $\{X_S, X_{S^c}\}$ refers to the full input vector X formed by concatenation. The reference distribution r is defined as:

$$r = r(X_{S^c}^l, X_{S^c}^r \mid X_S^l = x_S^l, X_S^r = x_S^r).$$

108 2.5 GENERALIZED PREFERENTIAL KERNEL[CHAU ET AL. (2022A)]
109110 **Definition 2.** Given a kernel $k : \mathcal{X} \times \mathcal{X} \rightarrow \mathbb{R}$, defined on the original feature space $\mathcal{X} \subseteq \mathcal{R}^d$, the
111 Generalized Preferential Kernel k_E is defined as:

112
$$k_E((x_i^l, x_i^r), (x_j^l, x_j^r)) = k(x_i^l, x_j^l) \cdot k(x_i^r, x_j^r) - k(x_i^l, x_j^r) \cdot k(x_i^r, x_j^l), \quad (5)$$

113

114 where the skew-symmetric function f is assumed to lie in the Reproducing Kernel Hilbert Space
115 ($RKHS$) \mathcal{H}_{k_E} associated with k_E .
116117 2.6 BLOCK STRUCTURE OF SHAPLEY VALUES
118119 One of the key properties satisfied by Shapley values, and more importantly for our purposes by Pref-
120 Shap, is the *efficiency* axiom which states that the sum of all feature attributions equals the overall
121 preference score. In particular, for a feature space of dimension d where features are grouped into
122 $d/2$ disjoint consecutive blocks of size 2, we have the following equation w.r.t. Pref-SHAP (Φ)(8):
123

124
$$\sum_{i=1}^{d/2} (\Phi_{2i-1} + \Phi_{2i}) = \sum_{i=1}^{d/2} (u_{2i-1}v_{2i} - u_{2i}v_{2i-1}) = u^\top Av, \quad (6)$$

125

126 where, $u, v \in \mathbb{R}^d$, d is even, and $A \in \mathbb{R}^{d \times d}$ is a block-diagonal matrix composed of $d/2$ skew-
127 symmetric 2×2 rotation matrices $\begin{bmatrix} 0 & -1 \\ 1 & 0 \end{bmatrix}$ as defined in (1). Each block corresponds to an anti-
128 symmetric interaction between two consecutive features. A natural question that arises is whether
129 Pref-SHAP also satisfies a finer-grained *block decomposition* property at the level of individual 2-
130 dimensional feature blocks. That is, for each odd index $i \in \{1, 3, \dots, d-1\}$, does the following
131 hold?
132

133
$$\Phi_i + \Phi_{i+1} = u_i v_{i+1} - u_{i+1} v_i = u^\top A_{i:i+1} v, \quad \text{for } i \bmod 2 \neq 0, \quad (7)$$

134

135 where $A_{i:i+1} \in \mathbb{R}^{d \times d}$ is a matrix whose only nonzero entries lie in a 2×2 skew-symmetric submatrix
136 spanning rows and columns i and $i+1$, and zeros elsewhere. Thus, the full matrix A can be written
137 as a sum of these block-local matrices: $A = \sum_{i=1}^{d/2} A_{2i-1:2i}$. Here, $A_{2i-1:2i}$ denotes the 2×2
138 submatrix of A corresponding to rows and columns $2i-1$ and $2i$. This structure leads us to ask:
139 under what conditions does Pref-SHAP decompose additively over such blocks, preserving the local
140 attribution property in Eq. equation 7?
141142 3 DOES PREF-SHAP OBEY THE BLOCK PATTERN?
143144 **Proposition 1** (Block Decomposition of Conditional Pref-SHAP under Independence). Consider
145 a skew-symmetric preference function $f : \mathcal{X} \times \mathcal{X} \rightarrow \mathbb{R}$ (Definition 1) defined on feature vectors
146 $u, v \in \mathbb{R}^d$, where the d features are partitioned into $d/2$ disjoint consecutive blocks: $B_j = \{2j-1, 2j\}$,
147 $j = 1, \dots, \frac{d}{2}$. Assume one of the following:
148149

- 150 • **Full independence:** All features $\{X_1, \dots, X_d\}$ are mutually independent, or
- 151 • **Blockwise independence:** Features within each block B_j may be dependent, but blocks are
152 mutually independent, i.e., $X_{B_i} \perp X_{B_j}$ for all $i \neq j$, where X_{B_j} denotes the features in
153 block B_j .

154 The preference function decomposes additively over blocks: $f(u, v) = \sum_{j=1}^{d/2} f_j(u_{B_j}, v_{B_j})$, where
155 each f_j depends only on features in block B_j .
156157 Pref-SHAP for feature $i \in [d]$ is analytically computed as
158

159
$$\Phi_i := \sum_{S \subseteq [d] \setminus \{i\}} \frac{|S|!(d-1-|S|)!}{d!} [\nu(S \cup \{i\}) - \nu(S)], \quad (8)$$

160

161 where the conditional value function is, $\nu(S) := \mathbb{E}[f(u, v) \mid (u_k, v_k)_{k \in S}]$.
162

162 Then, under the above assumptions, $\sum_{i \in B_j} \Phi_i = f_j(u_{B_j}, v_{B_j})$, for all $j = 1, \dots, \frac{d}{2}$. Moreover,
 163 the individual Pref-SHAP values Φ_i generally depend on the full feature set due to the global con-
 164 ditioning in v , but their sum over each block recovers the exact blockwise preference contribu-
 165 tion. If the features are correlated across blocks (i.e., the blockwise independence assumption fails), then
 166 this additive decomposition of the Pref-SHAP values does not generally hold.
 167

168 **Proof Sketch.** Consider features partitioned into blocks B_1, \dots, B_m . Pref-SHAP values are com-
 169 puted via differences of conditional expectations. Under full or blockwise independence, conditional
 170 expectations of features outside a block reduce to constants independent of conditioning subsets.
 171 Consequently, cross-block terms appear symmetrically in the Shapley difference terms and cancel
 172 out. This implies that Pref-SHAP values decompose additively over blocks, with each block's at-
 173 tribution depending only on its own features. In contrast, when features are arbitrarily correlated
 174 across blocks, these cancellations no longer occur, and the decomposition fails. The complete proof
 175 is provided in the appendix B.
 176

177 3.1 CAN OTHER SHAPLEY VARIANTS RECOVER BLOCK PATTERN(7)?

178 A natural question is whether using other value functions can help Pref-SHAP respect the canonical
 179 block structure in cases where the original conditional value function leads to violation. Specifically:
 180

181 **Off-manifold / Interventional / Marginal Shapley values**[Janzing et al. (2020)] evaluate features
 182 outside the data distribution, which may help remove interdependencies across blocks. However,
 183 such approaches lack robustness[Slack et al. (2020)] because they evaluate the model on unrealistic
 184 samples, potentially making the explanations unreliable and vulnerable to adversarial manipulation.

185 **ManifoldSHAP**[Taufiq et al. (2023)] attempts to stay on the data manifold by estimating it via kernel
 186 density estimators or score models. Since Pref-SHAP involves estimating conditional expectations
 187 from a distributional perspective, Kernel Mean Embeddings could serve as a tool for implementing
 188 ManifoldSHAP if applied in the Pref-SHAP context.

189 **Causal Shapley values**[Heskes et al. (2020)] incorporate the underlying causal graph and account
 190 for structural dependencies between features. This allows feature attribution to reflect true causal
 191 contributions, thereby improving interpretability over interventional or marginal approaches in the
 192 presence of feature correlation.

193 As an illustration, consider the Gaussian setup:

194 $X = [X_a, X_b]^T = [X_2, X_4, X_1, X_3]^T$, where $X_a = \{X_2, X_4\}$, and $X_b = \{X_1, X_3\}$.
 195 Assume $X \sim \mathcal{N}(\mu, \Sigma)$. The conditional expectation and covariance of X_a given X_b are as follows:
 196 $\mathbb{E}[X_a | X_b] = \mu_a + \Sigma_{ab}\Sigma_{bb}^{-1}(x_b - \mu_b)$, $\Sigma_{a|b} = \Sigma_{aa} - \Sigma_{ab}\Sigma_{bb}^{-1}\Sigma_{ba}$.
 197

198 Notably, the conditional mean does not depend on Σ_{aa} . This implies that even if features within
 199 a block (e.g., X_a) are highly correlated, their internal dependency does not affect the conditional
 200 expectation as long as X_b is fixed. However, dependency *across* blocks will break the block decom-
 201 position property under the conditional value function.

202 Hence, while conditional value functions capture statistical dependence, they may cause Pref-SHAP
 203 to violate canonical structure, leading to unintuitive or biased attributions, especially when sensitive
 204 features are involved. In such cases, alternative value functions like causal or manifold-based ones
 205 may provide more reliable and fair explanations.

207 3.2 CAN WE LEARN A FEATURE MAPPING TO RESTORE BLOCK STRUCTURE(7)?

209 We investigate whether it is possible to map the original features to a transformed space, such as an
 210 *eigenspace defined by the covariance matrix* so that the Pref-SHAP values exhibit a block structure
 211 in the transformed coordinates. Specifically, we consider an orthonormal linear transformation $W \in$
 212 $\mathbb{R}^{d \times d}$ such that $x = W^T u$, $y = W^T v$, where $u, v \in \mathbb{R}^d$ are original feature vectors, and $x, y \in \mathbb{R}^d$

213 are transformed features. $W = \begin{bmatrix} w_{11} & w_{21} & \cdots & w_{d1} \\ w_{12} & w_{22} & \cdots & w_{d2} \\ \vdots & \vdots & \ddots & \vdots \\ w_{1d} & w_{2d} & \cdots & w_{dd} \end{bmatrix}$, $u = Wx$, $v = Wy$ are the inverse

216 transformations .

217 Each transformed feature is, $x_i = \sum_{j=1}^d w_{ji}u_j$, $y_i = \sum_{j=1}^d w_{ji}v_j$, $\forall i = 1, \dots, d$.
218219 **Example: Skew-Symmetric Function with 4 Features** Consider the skew-symmetric preference
220 function $f(u, v) = u_1v_2 - u_2v_1 + u_3v_4 - u_4v_3$, which exhibits a natural block structure with two
221 blocks: $\{1, 2\}$ and $\{3, 4\}$.222 Expressing f in the transformed space,

224
$$f(u, v) = f(Wx, Wy) = (Wx)_1(Wy)_2 - (Wx)_2(Wy)_1 + (Wx)_3(Wy)_4 - (Wx)_4(Wy)_3$$

225
226
$$= \sum_{i,j=1}^d (w_{i1}w_{j2} - w_{i2}w_{j1} + w_{i3}w_{j4} - w_{i4}w_{j3}) (x_i y_j - x_j y_i).$$

227
228

229 Rearranging terms into differences of products (to maintain skew-symmetry), $f(x, y) =$
230 $\sum_{i < j} c_{ij} (x_i y_j - x_j y_i)$, where, $c_{ij} = w_{i1}w_{j2} - w_{i2}w_{j1} + w_{i3}w_{j4} - w_{i4}w_{j3}$.231 Due to the linear mixing by W , the original block structure (only interactions within blocks
232 $\{1, 2\}$ and $\{3, 4\}$) generally disappears. Instead, f becomes a *fully connected* skew-symmetric
233 form involving all pairs (i, j) of transformed features, where all c_{ij} can be nonzero. Hence, the
234 model in the transformed space no longer decomposes into independent blocks. Consequently,
235 the Pref-SHAP values computed on transformed features will not obey the block pattern seen in
236 the original features. This observation generalizes to higher dimensions and nonlinear models
237 with interaction terms: the orthonormal transform W mixes all features, distributing interactions
238 across transformed features. Nonlinear terms (e.g., products of features from different blocks) are
239 generally not diagonalized by W . Therefore, block independence is a property of the function
240 structure, not solely the feature covariance. Shapley values are generally not linear in the features
241 or their transformations, except for models based on a single item features. For such functions
242 that act on a single item, $f(u) = \beta^T u$, transforming features linearly as $x = W^T u$ yields
243 $f(u) = \beta^T u = \beta^T Wx = \tilde{\beta}^T x$, and Shapley values transform linearly: $\phi_{u_j} = \sum_i w_{ji} \phi_{x_i}$. For
244 *pairwise preference* models with feature interactions, this linearity breaks, and Shapley values of
245 original features cannot be represented as linear combinations of transformed features' Shapley
246 values.
247247 **Remark:** Mapping features to an eigenspace or another orthonormal basis does not, in general,
248 preserve the block independence structure of nonlinear interaction models like skew-symmetric
249 preference functions. Consequently, Pref-SHAP values computed in the transformed space will
250 reflect fully coupled feature interactions and fail to obey the original block pattern.
251252

4 STUDY OF PREF-SHAP PROPERTIES IN THE TWO-FEATURES SETTING

253254 When there are only two features, the analytical expression for Pref-SHAP(8) reduces to:
255

256
$$\Phi_1 = \frac{1}{2} [(u_1v_2 - u_2v_1) + u_1\mathbb{E}[Y_2|Y_1 = v_1] - v_1\mathbb{E}[X_2|X_1 = u_1]$$

257
$$- v_2\mathbb{E}[X_1|X_2 = u_2] + u_2\mathbb{E}[Y_1|Y_2 = v_2] - \mathbb{E}[X_1]\mathbb{E}[Y_2] + \mathbb{E}[Y_1]\mathbb{E}[X_2]]$$

258
259
$$\Phi_2 = \frac{1}{2} [(u_1v_2 - u_2v_1) - u_1\mathbb{E}[Y_2|Y_1 = v_1] + v_1\mathbb{E}[X_2|X_1 = u_1]$$

260
$$+ v_2\mathbb{E}[X_1|X_2 = u_2] - u_2\mathbb{E}[Y_1|Y_2 = v_2] - \mathbb{E}[X_1]\mathbb{E}[Y_2] + \mathbb{E}[Y_1]\mathbb{E}[X_2]] \quad (9)$$

261

262 Since $\mathbb{E}(X_i) = \mathbb{E}(Y_i) \forall i \in \{1, 2\}$, the last two terms vanish.
263264

4.1 IMPACT OF FEATURE VARIANCE ON PREF-SHAP

265266 Let us consider this analytically. Suppose the features are independent, then the Pref-SHAP values
267 simplify to:
268

269
$$\Phi_1 = \frac{1}{2} [(u_1v_2 - u_2v_1) + (u_1\mathbb{E}(Y_2)) - (v_1\mathbb{E}(X_2)) - (v_2\mathbb{E}(X_1)) + (u_2\mathbb{E}(Y_1))]$$

$$\Phi_2 = \frac{1}{2} [(u_1v_2 - u_2v_1) - (u_1\mathbb{E}(Y_2)) + (v_1\mathbb{E}(X_2)) + (v_2\mathbb{E}(X_1)) - (u_2\mathbb{E}(Y_1))] \quad (10)$$

Now, suppose, $\text{Var}(X_1) = \text{Var}(Y_1) = 100$ and $\text{Var}(X_2) = \text{Var}(Y_2) = 1$. Consider an instance where $u_1 = 100$, $v_1 = -100$, $u_2 = 1$, $v_2 = -1$. In this case, the first-order terms involving u_1 and v_1 dominate, so Φ_1 could be significantly larger than Φ_2 . However, for another instance with opposite signs (e.g., $u_1 = -100$, $v_1 = 100$, $u_2 = -1$, $v_2 = 1$), Φ_2 could become larger than Φ_1 .

Therefore, while individual Pref-SHAP values may be affected by the variance in the features, this effect can cancel out when averaging over many samples. In other words, the global (dataset-level) Pref-SHAP attributions are not directly biased by feature variance in expectation under independence. Hence, Pref-SHAP with conditional value functions represents the true conditional expectation of the model output. Thus, it does not directly encode feature variance. However, the uncertainty in prediction caused by high feature variance (especially in correlated settings) may influence the attribution in an indirect way. This distinction aligns with insights from information-theoretic approaches to attribution [Watson et al. (2024)], where variance influences model uncertainty but not necessarily marginal attributions unless the model or attribution method explicitly encodes that dependency.

4.2 EFFECT OF CONSTANT FEATURES ON PREF-SHAP

The full discussion with analysis is deferred to the appendix C due to space constraints. Briefly, even if a feature is constant across item pairs, it may still receive non-zero attribution under Pref-SHAP feature correlations. However, under certain independence assumptions and symmetry axiom, such features may yield equal attributions due to model structure.

Case	Baseline Form	$\Phi_1(\mathbf{9})$
1	$z = \frac{u+v}{2}$ (Pair-specific baseline)	$\frac{1}{2}(u_1v_2 - u_2v_1 + u_1u_2 - v_1v_2)$
2	$z = \mathbb{E}[Z]$ (Global baseline)	$\frac{1}{2}(u_1v_2 - u_2v_1 + (u_1 - v_1)\mathbb{E}[Z_2] - (v_2 - u_2)\mathbb{E}[Z_1])$

Figure 1: Comparison of Baseline Shapley Forms

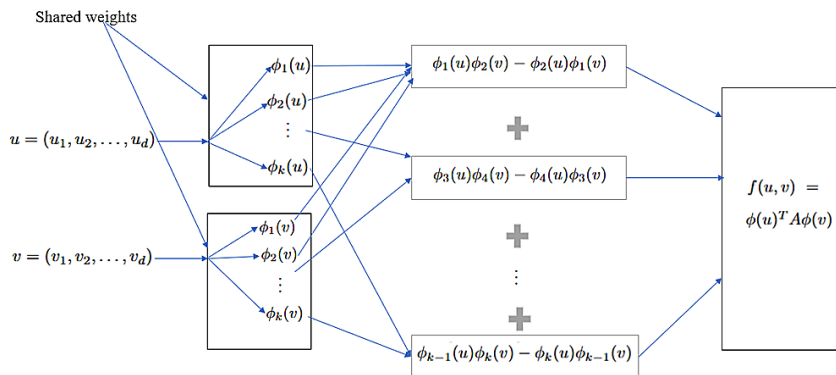
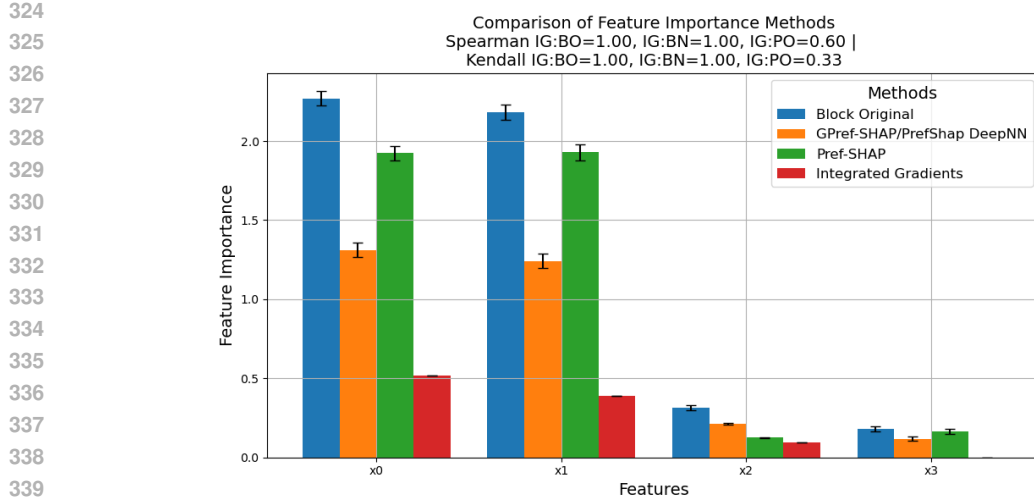


Figure 2: Generalized Pref-SHAP architecture using a simple neural network

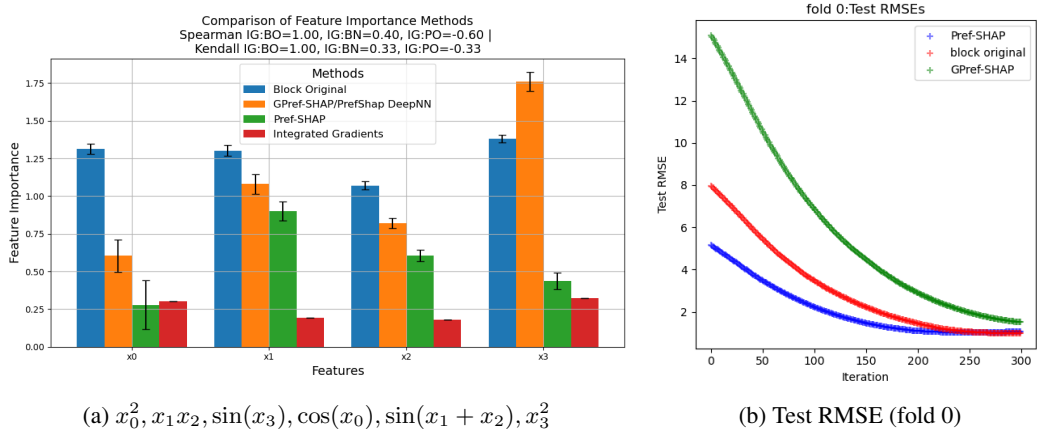
4.3 PREF-SHAP VS. BASELINE SHAPLEY[SUNDARARAJAN & NAJMI (2020)]

$$\text{Baseline } z = (z_1, z_2) = \left(\frac{u_1 + v_1 + \dots}{n}, \frac{u_2 + v_2 + \dots}{n} \right) = (\mathbb{E}[Z_1], \mathbb{E}[Z_2]) \quad (11)$$

In Case 1(Fig. 1), when features are equal, attribution vanishes. In Case 2, even equal features may have non-zero attribution if they deviate from the global baseline $\mathbb{E}[Z]$. Pref-SHAP resembles Case 2 and better accounts for meaningful deviations from population averages.



341 Figure 3: Quadratic feature mappings $\{x_0^2, x_1^2, x_0x_1, x_0x_2\}$. Generalized Pref-SHAP is abbreviated as **GPref-SHAP**; **IG** = Integrated Gradients, **BO** = Block Original, **BN** = Block DeepNN, and **PO** = Pref-SHAP Original. **IG:BO** means the rank correlation between them. The terms **Pref-SHAP DeepNN** and **Block DeepNN** are used interchangeably to refer to GPref-SHAP. Terms in the captions represent the mapped features.



360 Figure 4: (a)hybrid mapping of features, (b) ReLU network (4 input features, 6 mapped features, 4 hidden
361 layers, 16 nodes in each layer).

5 GENERALIZED PREFERENTIAL KERNEL(5) INSIGHT:

Given the bilinear form of the *Generalized Preferential kernel*[Chau et al. (2022a)]:

$$\sum_{i=1}^n \alpha_i K_E((x_i, y_i), (x_{\text{test}}, y_{\text{test}})) = x_{\text{test}}^\top \left(\sum_{i=1}^n \alpha_i (x_i y_i^\top - y_i x_i^\top) \right) y_{\text{test}}. \quad (12)$$

the model output becomes a bilinear form over input pairs with *weights represented by a skew-symmetric matrix i.e. $\sum_{i=1}^n \alpha_i (x_i y_i^\top - y_i x_i^\top)$ in a transformed space*. This naturally aligns with the *linear kernel* as the base kernel (instead of *RBF kernel*), which is both expressive and computationally efficient in this context, i.e. in cases where the feature map ϕ is the identity function.

Effective Feature Space for Pref-SHAP: In this formulation, the prediction function is linear in the space of effective features, which are formed as pairwise interactions of the original features. As each pair of features (x_i, x_j) contributes an interaction term, the number of effective features becomes $\binom{d}{2}$, significantly expanding the representational capacity. The final prediction is thus: $f(u, v) = \sum_{i < j} \alpha_{ij} (u_i v_j - u_j v_i)$, where α_{ij} are the learned coefficients associated with each

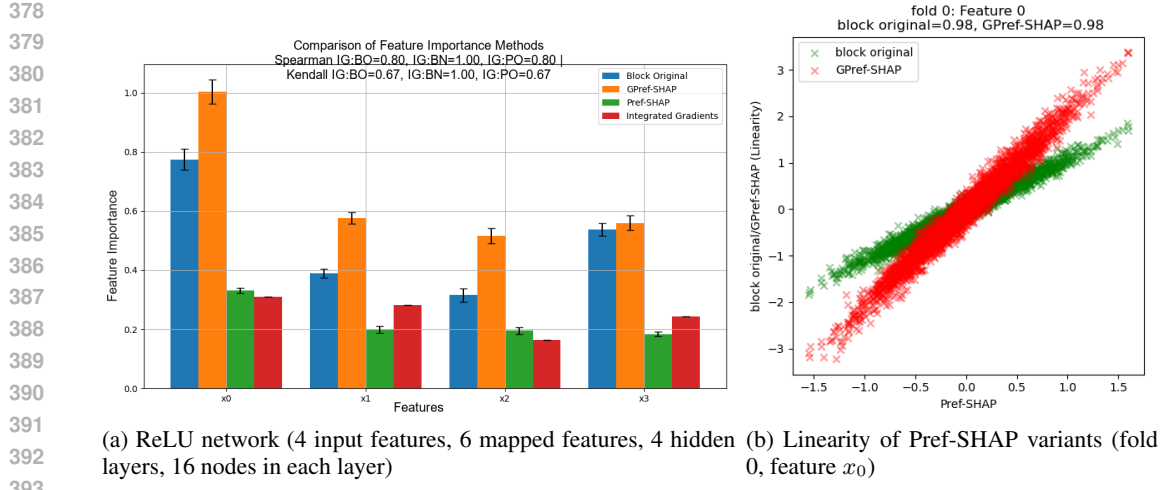


Figure 5: ReLU network

interaction. This formulation allows us to attribute importance to each original feature based on the strength and frequency of its interactions across data instances.

6 PROPOSED FRAMEWORK: GENERALIZED PREF-SHAP (2)

Algorithm 1 Generalized Pref-SHAP

Input: Pairwise item data $\{X_l, X_r, Y\}$ with features $X \in \mathbb{R}^d$, number of blocks k for feature mapping.

1. Learn the unknown feature mapping $\phi = (\phi_1, \phi_2, \dots, \phi_k)(2)$ using the neural network shown in Figure 2, where the predicted output is: $f(x_l, x_r) = \phi(x_l)^T A \phi(x_r) = \sum_{i=1}^{k/2} (\phi_{2i-1}(x_l) \phi_{2i}(x_r) - \phi_{2i}(x_l) \phi_{2i-1}(x_r))$.
2. Construct $k/2$ datasets, each corresponding to a blockwise pairwise interaction of mapped features using ϕ .
3. For each block dataset, apply Kernel Ridge Regression (KRR) to learn a component function.
4. Compute the residual between the original label Y and the sum of predictions from all $k/2$ component models. Apply KRR to this residual dataset.
5. Compute Pref-SHAP values for each of the $k/2$ blocks and the residual component, giving a $k \times (k/2 + 1)$ matrix of attributions.
6. Aggregate feature attributions by summing across columns (i.e., summing attributions across blocks for each feature).

Output: Final Pref-SHAP value for each original input feature.

In standard Pref-SHAP, the model approximates the skew-symmetric function of the mapped features using Kernel Ridge Regression (KRR) but does not learn the mapping $\phi(2)$ explicitly. Consequently, it cannot exploit the canonical block structure inherent to skew-symmetric functions. In contrast, our proposed *Generalized Pref-SHAP* explicitly learns the feature mapping $\phi(2)$, enabling a structured decomposition of the preference function into interpretable blocks. This decomposition preserves the block structure of the underlying function and facilitates more accurate and meaningful feature attributions. By jointly learning the feature representation and maintaining block-wise interpretability, *Generalized Pref-SHAP* improves the transparency and faithfulness of the attribution process, aligning explanations more closely with the structure of the learned model.

The network takes as input a pair of items represented using their original features and learns the feature mappings of each item via weight sharing. The learned mappings are then passed into a

432 module which computes the skew-symmetric preference function for these mapped features. The
 433 detailed explanation of the algorithmic steps are described in appendix A.
 434

435 **7 EXPERIMENTS**
 436

437 In this section, we describe our experimental setup and results on both synthetic and real-world
 438 datasets. We have conducted experiments mainly on carefully generated synthetic data because
 439 the motivation behind Generalized Pref-SHAP is rooted in the design of feature mappings $\phi(2)$, and
 440 real-world datasets rarely provide a ground truth for global feature importance. However, in domains
 441 where expert knowledge about feature relevance exists, real-data experiments can help identify the
 442 more interpretable model. It is quite possible that the explicit features in the real data get mapped
 443 to some hidden space before applying the skew-symmetric preference function instead of directly
 444 contributing to the preferences and this phenomenon can be better explained through our proposed
 445 method.
 446

447 **7.1 SYNTHETIC AND REAL-WORLD EXPERIMENTS**
 448

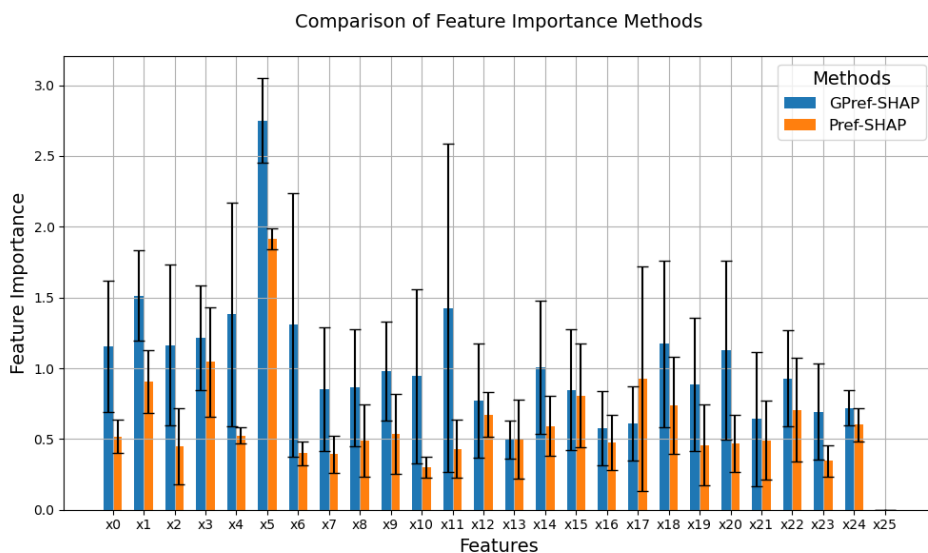
449 We conduct experiments using synthetic data consisting of $n = 100$ items, where each item's fea-
 450 tures are sampled from a 4-dimensional Gaussian distribution with mean zero and identity covari-
 451 ance: $x_i \sim \mathcal{N}(0, \mathbf{I})$ for $i = 1, \dots, 100$. We construct preference labels using various differentiable
 452 feature mappings ϕ , including:

453 **Polynomial mappings:** quadratic expansions, **Sinusoidal mappings:** combinations of $\sin(\cdot)$, $\cos(\cdot)$
 454 applied to linear projections, **Hybrid mappings:** combinations of polynomial and sinusoidal trans-
 455 formations, **Neural network mappings:** small feedforward networks with ReLU activations and
 456 varying depth/width.

457 The preference labels are generated by applying the skew-symmetric function f to transformed
 458 features. We evaluate the feature importance scores computed using four methods: **Pref-SHAP:**
 459 the original method using conditional Shapley values on learned KRR models. **Generalized Pref-**
 460 **SHAP (Ours):** learns each skew-symmetric component block via neural networks, then aggregates
 461 their Shapley values. **Integrated Gradients (Baseline):** standard attribution baseline for differ-
 462 entiable models. **Block-Original:** a reference method that trains separate KRR models per block and
 463 aggregates block-level Pref-SHAP values.

464 For the ground truth, we compute the global feature importance scores with respect to the feature
 465 mapping function using *Integrated Gradients*, and then propagate those scores to the canonical skew-
 466 symmetric preference function. Since each block in the canonical form contains exactly two terms,
 467 with each feature appearing once per term, the importance score of each feature is doubled per block.
 468 As the blocks are disjoint, the final feature importance is obtained by summing these contributions
 469 across blocks. This enables comparison using rank-based metrics. We use all $\binom{100}{2}$ unique pairs
 470 for training and evaluation, as the task is regression-based whereas our real-world experiment is
 471 based on classification of pairwise preferences. The pairwise comparisons with labels are split into
 472 training (80%), validation (10%), and test (10%) sets and the experiments are averaged over 5 folds.
 473 Feature attribution is computed on a randomly selected subset of the pairwise data. For Kernel Ridge
 474 Regression, hyperparameter tuning is performed via gradient-based optimization using the *Falkon*
 475 library. For the neural network setup, we fix two hidden layers and employ Bayesian optimization
 476 using *Optuna* with 100 trials to tune the hyperparameters: the number of hidden nodes (shared
 477 across layers) is selected from the set $\{32, 64, 96, 128\}$, while the learning rate and weight decay
 478 are sampled from logarithmic ranges $[10^{-4}, 10^{-1}]$ and $[10^{-6}, 10^{-2}]$ respectively. We use the mean
 479 squared error (MSE) loss and optimize using the Adam optimizer with a batch size of 64 and early
 480 stopping based on validation loss. *Real-world* experiment (6) is based on classification, so Kernel
 481 Logistic Regression (KLR) is used for modeling the pairwise preferences and the concept of residue
 482 modeling is not applicable here. We have used the publicly available dataset *Pokemon*(Nguyen
 483 Van Anh (2021)) for the same. The 25 features are mapped into 4 hidden features and applied the
 484 skew symmetric function separately on the 2 blocks generated from the mapped features.

485 **Evaluation Metrics:** We report three types of plots for each setup: *Bar plots*: Global feature
 486 importance scores (averaged absolute attribution values across test samples) for each method. *Spear-*
 487 *man and Kendall Tau rank correlations* between each method's global feature importance scores
 488 and the ground truth (or baseline Integrated Gradients) are computed. *Linearity plots*: Scatter-



540 REFERENCES
541

542 Amanda Bower and Laura Balzano. Preference modeling with context-dependent salient features.
543 In *International Conference on Machine Learning*, pp. 1067–1077. PMLR, 2020.

544 Siu Lun Chau, Javier Gonzalez, and Dino Sejdinovic. Learning inconsistent preferences with gaus-
545 sian processes. In *International Conference on Artificial Intelligence and Statistics*, pp. 2266–
546 2281. PMLR, 2022a.

547 Siu Lun Chau, Robert Hu, Javier Gonzalez, and Dino Sejdinovic. Rkhs-shap: Shapley values for
548 kernel methods. *Advances in neural information processing systems*, 35:13050–13063, 2022b.

549 Shuo Chen and Thorsten Joachims. Modeling intransitivity in matchup and comparison data. In
550 *Proceedings of the ninth acm international conference on web search and data mining*, pp. 227–
551 236, 2016.

552 Fabian Fumagalli, Maximilian Muschalik, Patrick Kolpaczki, Eyke Hüllermeier, and Barbara Ham-
553 mer. Kernelshap-iq: Weighted least-square optimization for shapley interactions. *arXiv preprint*
554 *arXiv:2405.10852*, 2024.

555 Steffen Grünewälder, Guy Lever, Luca Baldassarre, Sam Patterson, Arthur Gretton, and Mas-
556 similano Pontil. Conditional mean embeddings as regressors-supplementary. *arXiv preprint*
557 *arXiv:1205.4656*, 2012.

558 Tom Heskes, Evi Sijben, Ioan Gabriel Bucur, and Tom Claassen. Causal shapley values: Exploit-
559 ing causal knowledge to explain individual predictions of complex models. *Advances in neural*
560 *information processing systems*, 33:4778–4789, 2020.

561 Robert Hu, Siu Lun Chau, Jaime Ferrando Huertas, and Dino Sejdinovic. Explaining preferences
562 with shapley values. *Advances in Neural Information Processing Systems*, 35:27664–27677,
563 2022.

564 Dominik Janzing, Lenon Minorics, and Patrick Blöbaum. Feature relevance quantification in ex-
565 plainable ai: A causal problem. In *International Conference on artificial intelligence and statis-
566 tics*, pp. 2907–2916. PMLR, 2020.

567 Rahul Makhijani and Johan Ugander. Parametric models for intransitivity in pairwise rankings. In
568 *The World Wide Web Conference*, pp. 3056–3062, 2019.

569 Sahand Negahban, Sewoong Oh, and Devavrat Shah. Rank centrality: Ranking from pair-wise
570 comparisons, 2015.

571 Tuan Nguyen Van Anh. Pokémon dataset with team combat. <https://www.kaggle.com/datasets/tuannguyenvananh/pokemon-dataset-with-team-combat>, 2021.
572 Accessed: 2025-09-23.

573 Arun Rajkumar and Shivani Agarwal. When can we rank well from comparisons of $O(n \log(n))$
574 non-actively chosen pairs? In *Conference on Learning Theory*, pp. 1376–1401. PMLR, 2016.

575 Arun Rajkumar, Vishnu Veerathu, and Abdul Badey Mir. A theory of tournament representations.
576 *arXiv preprint arXiv:2110.05188*, 2021.

577 Lloyd S Shapley et al. A value for n-person games. 1953.

578 Dylan Slack, Sophie Hilgard, Emily Jia, Sameer Singh, and Himabindu Lakkaraju. Fooling lime
579 and shap: Adversarial attacks on post hoc explanation methods. In *Proceedings of the AAAI/ACM*
580 *Conference on AI, Ethics, and Society*, pp. 180–186, 2020.

581 Mukund Sundararajan and Amir Najmi. The many shapley values for model explanation. In *Inter-
582 national conference on machine learning*, pp. 9269–9278. PMLR, 2020.

583 Mukund Sundararajan, Kedar Dhamdhere, and Ashish Agarwal. The shapley taylor interaction
584 index. In *International conference on machine learning*, pp. 9259–9268. PMLR, 2020.

594 Muhammad Faaiq, Patrick Blöbaum, and Lenon Minorics. Manifold restricted interventional
 595 shapley values. In *International Conference on Artificial Intelligence and Statistics*, pp. 5079–
 596 5106. PMLR, 2023.

597 Vishnu Veerathu and Arun Rajkumar. On the structure of parametric tournaments with application
 598 to ranking from pairwise comparisons. *Advances in Neural Information Processing Systems*, 34:
 599 12065–12076, 2021.

600 David Watson, Joshua O’Hara, Nick Tax, Richard Mudd, and Ido Guy. Explaining predictive un-
 601 certainty with information theoretic shapley values. *Advances in Neural Information Processing
 602 Systems*, 36, 2024.

605 A APPENDIX

606 Detailed Explanation of the Algorithm Steps:

- 607 **1. Learning the Feature Mapping ϕ :** The algorithm begins by learning a feature mapping
 608 $\phi = (\phi_1, \phi_2, \dots, \phi_k)$ via a neural network architecture (illustrated in Figure 2). This net-
 609 work takes as input a pair of items (x_l, x_r) with original features in \mathbb{R}^d , and outputs their
 610 transformed features. The learned mapping ϕ is structured to reflect the block-wise decom-
 611 position, where each pair (ϕ_{2i-1}, ϕ_{2i}) corresponds to a canonical 2×2 skew-symmetric
 612 block. This decomposition explicitly encodes the skew-symmetric structure in the feature
 613 space.
- 614 **2. Constructing Blockwise Datasets:** After learning the feature mappings, the dataset is
 615 partitioned into $k/2$ separate block datasets, each corresponding to the pairwise interaction
 616 between the mapped features ϕ_{2i-1} and ϕ_{2i} . These datasets isolate the contribution of each
 617 skew-symmetric block to the overall preference prediction.
- 618 **3. Fitting Kernel Ridge Regression (KRR) Models:** For each block dataset, Kernel Ridge
 619 Regression is applied to learn a component function that models the preference contribu-
 620 tion from that specific block. KRR allows flexible, nonparametric fitting that captures the
 621 potentially complex relationships within each block.
- 622 **4. Modeling the Residual:** The sum of predictions from all blockwise KRR models provides
 623 a partial reconstruction of the original preference function. This approximation may not
 624 capture all nuances of the data, particularly nonlinearities or interactions not aligned with
 625 the learned blocks. We compute the residual as the difference between the true labels Y
 626 and the aggregated predictions from the blockwise models, thereby capturing information
 627 not explained by the canonical blocks. A separate KRR model is then fit to this residual
 628 dataset, enabling the method to recover additional signal beyond what is captured by the
 629 blockwise decomposition.
- 630 **5. Computing Pref-SHAP Values:** Pref-SHAP values are computed individually for each of
 631 the $k/2$ block component models and the residual model. This yields a matrix of attribu-
 632 tions of size $k \times (k/2 + 1)$, where each column corresponds to a block (or residual), and
 633 each row corresponds to one of the k mapped features. These attributions represent the
 634 contribution of each mapped feature within its block to the preference prediction.
- 635 **6. Aggregating Feature Attributions:** Finally, to obtain the attributions for the original in-
 636 put features, the algorithm sums the Pref-SHAP values across all blocks and the residual
 637 for each original feature. This aggregation consolidates the blockwise contributions and
 638 residual effects into a single attribution score per feature, reflecting the overall importance
 639 of each input feature in driving the preference decisions.

642 B PROPOSITION 1

644 *Proof.* We prove the proposition in three steps: base case $d = 4$, generalization to arbitrary even d ,
 645 and failure of decomposition under correlation.

646 **Step 1: Base case ($d = 4$)**

648 Partition features into two blocks:
 649

$$650 \quad B_1 = \{1, 2\}, \quad B_2 = \{3, 4\}.$$

651 By assumption, the preference function decomposes additively:
 652

$$653 \quad f(u, v) = f_1(u_{B_1}, v_{B_1}) + f_2(u_{B_2}, v_{B_2}).$$

654 For feature $i = 1$, the Pref-SHAP value is
 655

$$656 \quad \Phi_1 = \sum_{S \subseteq \{2, 3, 4\}} w(S) [\nu(S \cup \{1\}) - \nu(S)], \quad w(S) := \frac{|S|!(3 - |S|)!}{4!}.$$

659 By linearity of expectation,
 660

$$661 \quad \nu(S) = \mathbb{E}[f(u, v) \mid (u_k, v_k)_{k \in S}] = \mathbb{E}[f_1 \mid S] + \mathbb{E}[f_2 \mid S].$$

662 Blockwise independence implies that conditioning factorizes:
 663

$$664 \quad \mathbb{E}[f_j \mid S] = \mathbb{E}[f_j \mid S \cap B_j], \quad j = 1, 2.$$

666 Since $1 \in B_1$, the marginal contribution satisfies
 667

$$668 \quad \nu(S \cup \{1\}) - \nu(S) = [\nu_1((S \cup \{1\}) \cap B_1) - \nu_1(S \cap B_1)] + 0,$$

669 because $(S \cup \{1\}) \cap B_2 = S \cap B_2$ and f_2 does not change.
 670

671 Decompose S as $S = S_1 \cup S_2$, where
 672

$$673 \quad S_1 = S \cap B_1 \subseteq \{2\}, \quad S_2 = S \cap B_2 \subseteq \{3, 4\}.$$

674 Then,
 675

$$676 \quad \Phi_1 = \sum_{S_1 \subseteq \{2\}} \sum_{S_2 \subseteq \{3, 4\}} w(S_1 \cup S_2) [\nu_1(S_1 \cup \{1\}) - \nu_1(S_1)].$$

677 The marginal contribution depends only on S_1 , so
 678

$$679 \quad \Phi_1 = \sum_{S_1 \subseteq \{2\}} [\nu_1(S_1 \cup \{1\}) - \nu_1(S_1)] \underbrace{\sum_{S_2 \subseteq \{3, 4\}} w(S_1 \cup S_2)}_{\text{weight sum}}.$$

683 By the combinatorial properties of Shapley weights, the inner sum over S_2 equals the Shapley weight
 684 on block B_1 :
 685

$$686 \quad \sum_{S_2 \subseteq \{3, 4\}} w(S_1 \cup S_2) = \frac{|S_1|!(|B_1| - 1 - |S_1|)!}{|B_1|!} = \frac{|S_1|!(1 - |S_1|)!}{2!}.$$

689 Thus,
 690

$$691 \quad \Phi_1 = \sum_{S_1 \subseteq \{2\}} \frac{|S_1|!(1 - |S_1|)!}{2!} [\nu_1(S_1 \cup \{1\}) - \nu_1(S_1)].$$

693 Applying the same argument to feature 2, and then summing $\Phi_1 + \Phi_2$ yields
 694

$$695 \quad \Phi_1 + \Phi_2 = f_1(u_{B_1}, v_{B_1}).$$

696 Similarly, $\Phi_3 + \Phi_4 = f_2(u_{B_2}, v_{B_2})$.
 697

698 **Step 2: Generalization to arbitrary even d**
 699

700 For $i \in B_j$, decompose any subset $S \subseteq [d] \setminus \{i\}$ as
 701

$$S = S_j \cup S_{-j}, \quad S_j \subseteq B_j \setminus \{i\}, \quad S_{-j} \subseteq [d] \setminus (B_j \cup \{i\}).$$

702 Using linearity,

$$703 \\ 704 \quad \nu(S) = \sum_{m=1}^{d/2} \nu_m(S \cap B_m). \\ 705 \\ 706$$

707 By blockwise independence,

$$708 \quad \nu_m(S \cap B_m) = \nu_m(S_j \cap B_m) \quad \text{if } m = j, \\ 709$$

710 and conditioning on S_{-j} does not affect ν_j .

711 Hence,

$$712 \quad \nu(S \cup \{i\}) - \nu(S) = \nu_j(S_j \cup \{i\}) - \nu_j(S_j). \\ 713$$

714 Then,

$$715 \quad \Phi_i = \sum_{S_j \subseteq B_j \setminus \{i\}} \sum_{S_{-j}} w(S_j \cup S_{-j}) [\nu_j(S_j \cup \{i\}) - \nu_j(S_j)]. \\ 716 \\ 717$$

718 Marginal contributions depend only on S_j , so summing weights over S_{-j} gives

$$719 \quad \sum_{S_{-j}} w(S_j \cup S_{-j}) = \frac{|S_j|! (|B_j| - 1 - |S_j|)!}{|B_j|!}, \\ 720 \\ 721$$

722 the Shapley weight inside block B_j .

723 Therefore,

$$724 \quad \Phi_i = \sum_{S_j \subseteq B_j \setminus \{i\}} \frac{|S_j|! (|B_j| - 1 - |S_j|)!}{|B_j|!} [\nu_j(S_j \cup \{i\}) - \nu_j(S_j)]. \\ 725 \\ 726$$

727 Summing over all $i \in B_j$,

$$728 \quad \sum_{i \in B_j} \Phi_i = f_j(u_{B_j}, v_{B_j}). \\ 729 \\ 730$$

731 **Special Case: Full Independence.** When all features are mutually independent (i.e., each feature forms its own block), the block decomposition reduces to:

$$732 \quad f(u, v) = \sum_{j=1}^d f_j(u_j, v_j), \\ 733 \\ 734$$

735 with $B_j = \{j\}$. Since each block now contains only one feature, the Pref-SHAP attribution for
736 feature i becomes:

$$737 \quad \Phi_i = \nu_i(\{i\}) - \nu_i(\emptyset) = f_i(u_i, v_i),$$

738 because the Shapley value over a singleton block reduces to the full contribution of that feature.
739 Thus, Pref-SHAP values are fully local and additive over individual features, and the global attribu-
740 tion decomposes as:

$$741 \quad \sum_{i=1}^d \Phi_i = f(u, v). \\ 742 \\ 743$$

744 This recovers the case of *full additivity* and *local interpretability* under complete feature indepen-
745 dence.

746 Step 3: Necessity and failure under correlation

747 If features are correlated across blocks, the conditional expectation does not factorize:

$$748 \quad \mathbb{E}[f_j | S] \neq \mathbb{E}[f_j | S \cap B_j]. \\ 749$$

750 Thus,

$$751 \quad \nu(S \cup \{i\}) - \nu(S)$$

depends on conditioning on features outside B_j .

This breaks the factorization of Shapley weights and the blockwise decomposition of Pref-SHAP values fails.

Remark:

The Shapley value's symmetry axiom ensures that features with identical marginal contributions receive equal attribution, enabling cancellation of terms corresponding to conditioning on outside blocks when independence holds.

Linearity of expectation and combinatorial properties of weights guarantee that summation over subsets outside a block sums to one, allowing the reduction of sums to blockwise Shapley values.

This combination of linearity, independence, and symmetry underpins the blockwise decomposition of Pref-SHAP values.

□

C STUDY OF PREF-SHAP PROPERTIES W.R.T THE CANONICAL FORM

C.1 EFFECT OF CONSTANT FEATURES ON PREF-SHAP

- Consider a skew-symmetric function with features $u = [u_1, u_2]$, $v = [v_1, v_2]$, where each item is drawn from a bivariate Gaussian distribution with zero mean:

$$Z_1 = [X_1, Y_1]^\top, \quad Z_2 = [X_2, Y_2]^\top, \quad Z_1, Z_2 \sim \mathcal{N}(0, \Sigma).$$

From (10), as $\mathbb{E}[X_i] = \mathbb{E}[Y_i]$, $\forall i$, we find $\Phi_1 \neq \Phi_2$ in general. Even if $\mathbb{E}[X_i] = \mathbb{E}[X_j] \forall i, j$, Φ_1 and Φ_2 differ unless additional constraints hold.

- Even when one feature is kept constant (e.g., $u_2 = v_2$), it may still receive a nonzero Shapley value. For example:

$$\Phi_1 = \frac{1}{2}(u_1 - v_1)(u_2 + \mathbb{E}[X_1]), \quad \Phi_2 = \frac{1}{2}(u_1 - v_1)(u_2 - \mathbb{E}[X_1]).$$

If $u_2 = v_2 = \mathbb{E}[X_1]$, then $\Phi_2 = 0$, but $\Phi_1 = f(u, v)$.

- If $\mathbb{E}[X_1] = 0$, then $\Phi_1 = \Phi_2 = \frac{1}{2}(u_1 - v_1)u_2$. Thus, the Shapley values are equal, and this equality is due to the *symmetry axiom*. The symmetry axiom states that two features should receive equal Shapley values if they contribute equally across all coalitions. For the two-feature case, if $v(\{1\}) = v(\{2\}) \Rightarrow \Phi_1 = \Phi_2$, even when one of the features is held constant.

- To explore this further, define:

$$v(\{1\}) = \frac{1}{2}(u_1 \mathbb{E}[Y_2 | Y_1 = v_1] - v_1 \mathbb{E}[X_2 | X_1 = u_1]),$$

$$v(\{2\}) = \frac{1}{2}(v_2 \mathbb{E}[X_1 | X_2 = u_2] - u_2 \mathbb{E}[Y_1 | Y_2 = v_2]).$$

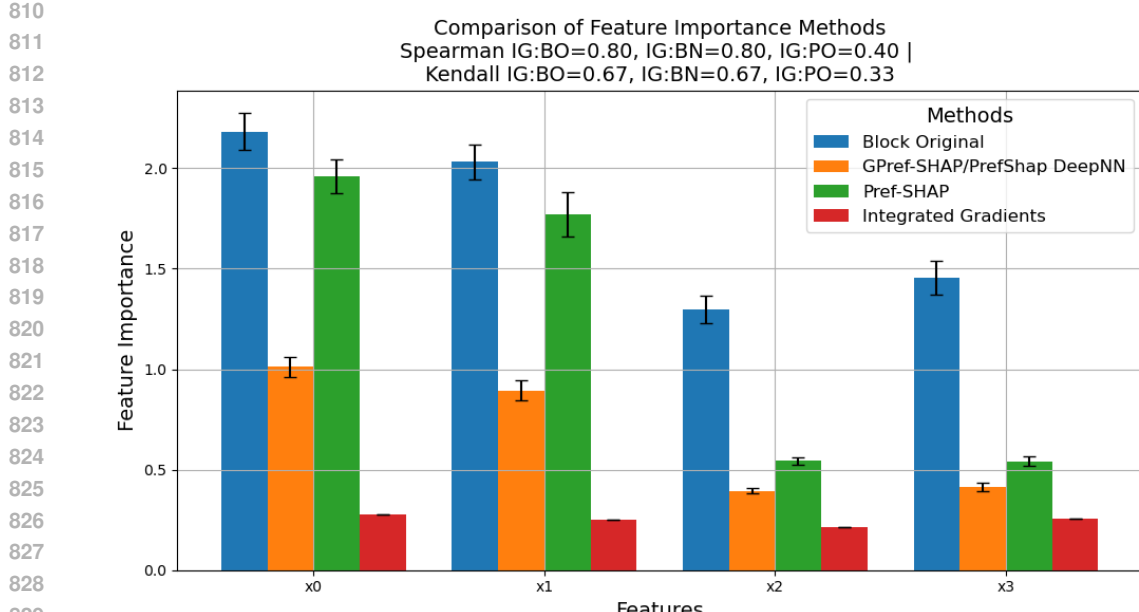
If the features are independent, the conditional expectations reduce to marginals, and equality $v(\{1\}) = v(\{2\})$ implies:

$$(u_1 - v_1)\mathbb{E}[X_2] = (v_2 - u_2)\mathbb{E}[X_1] \tag{13}$$

If $\mathbb{E}[X_1] = \mathbb{E}[X_2] = 0$, then $\Phi_1 = \Phi_2$ always. But, if $\mathbb{E}[X_1] = \mathbb{E}[X_2] \neq 0$, then

$$\begin{aligned} \Phi_1 = \Phi_2 \implies u_1 - v_1 &= v_2 - u_2 \\ \implies u_1 + u_2 &= v_1 + v_2 \end{aligned} \tag{14}$$

- This may appear counterintuitive: the constant feature may get equal attribution even though it does not vary. This is not an artifact of the conditional expectation but a consequence of the symmetry axiom. Even if a feature is constant or non-informative in terms of variation, Pref-SHAP may still assign it equal attribution simply due to how it appears in the function and due to symmetry, unless the distribution is shifted. This suggests, Pref-SHAP attributions are not just about feature importance in terms of variance or marginal effect, but also about how the feature interacts structurally in the model and in the coalitional expectations.

Figure 7: $x_0^2, x_1^2, x_2^2, x_3^2$

- The model function $f(u, v) = u^\top Av$ involves pairwise products of features (e.g., $u_1v_2 - u_2v_1$). Thus, the contribution of one feature depends on its interaction with the other. A constant feature interacting with a varying one may still result in a nonzero attribution.
- This motivates the use of *Pairwise Interaction Shapley values*[Sundararajan et al. (2020), Fumagalli et al. (2024)], which quantify pairwise contributions directly. Interaction Shapley methods can attribute the output more intuitively in models where the output depends primarily on feature interactions, as is the case in skew-symmetric functions. These interactions are model-driven, and statistical correlation (e.g., in the Gaussian setting) further modulates their effect when conditional value functions are used.

D ADDITIONAL SYNTHETIC DATA

We also conduct experiments using synthetic data consisting of $n = 100$ items, where each item's features are sampled from a 4-dimensional Gaussian distribution with zero mean and a covariance matrix whose diagonal entries are 1 and off-diagonal entries are 0.7:

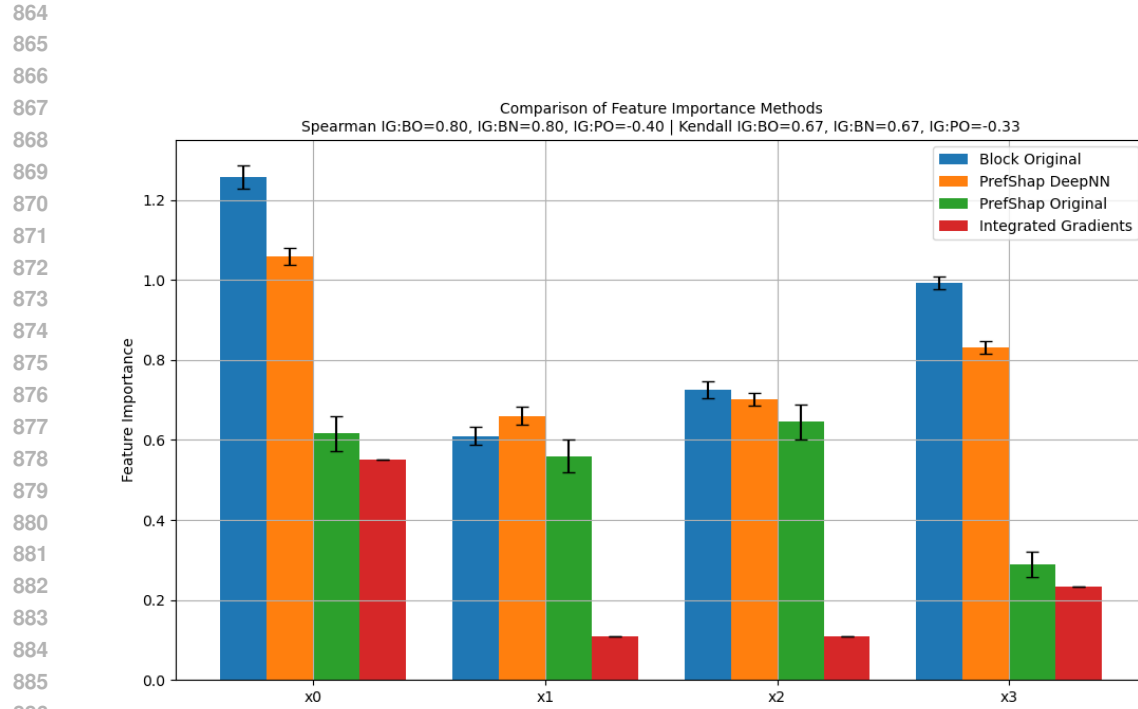
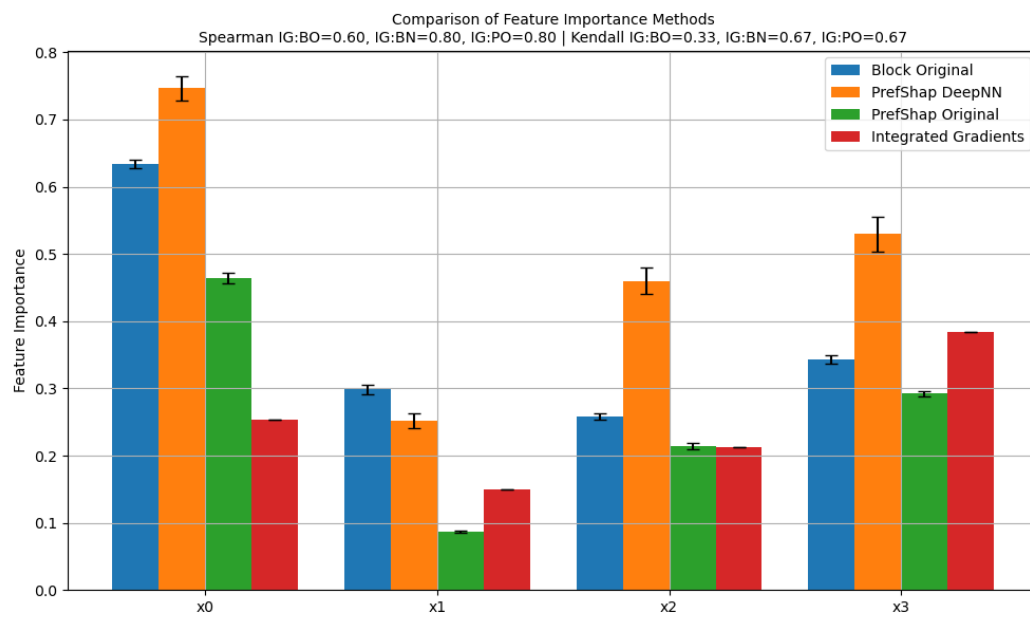
$$x^{(i)} \sim \mathcal{N}(0, \Sigma), \quad \text{for } i = 1, \dots, 100,$$

where $\Sigma_{jj} = 1$ and $\Sigma_{jk} = 0.7$ for $j \neq k$.

Figures 14, 15 and 16 are the synthetic experiments conducted on such highly correlated data. If we compare figures 16 and 17, we can see that when the features are highly correlated, the dummy/inactive feature x_3 gets more attribution than the case when the features are independent.

D.1 SANITY CHECK

Figures 17, 18, 19, 20 are some experiments used for sanity check. In figure 17, the fourth/last feature is not used for generating mapped features and hence the skew-symmetric function. In figures 18, 19 and 20 items are generated using a 6-dimensional Gaussian distribution with mean zero and identity covariance: $x_i \sim \mathcal{N}(0, \mathbf{I})$ for $i = 1, \dots, 100$, but only the first 4 features are used for feature mapping and label generation, so the last two features act like dummy ones. We can observe from these plots that the dummy features get zero attribution in case of *Integrated Gradients* whereas Block Original and Generalized Pref-SHAP have nearly-zero or the lowest attribution for

Figure 8: $x_0^2, x_1 x_2, \sin(x_3), \cos(x_0)$ Figure 9: $\sin(x_0), \cos(x_1), \sin(2x_2), \cos(2x_3)$

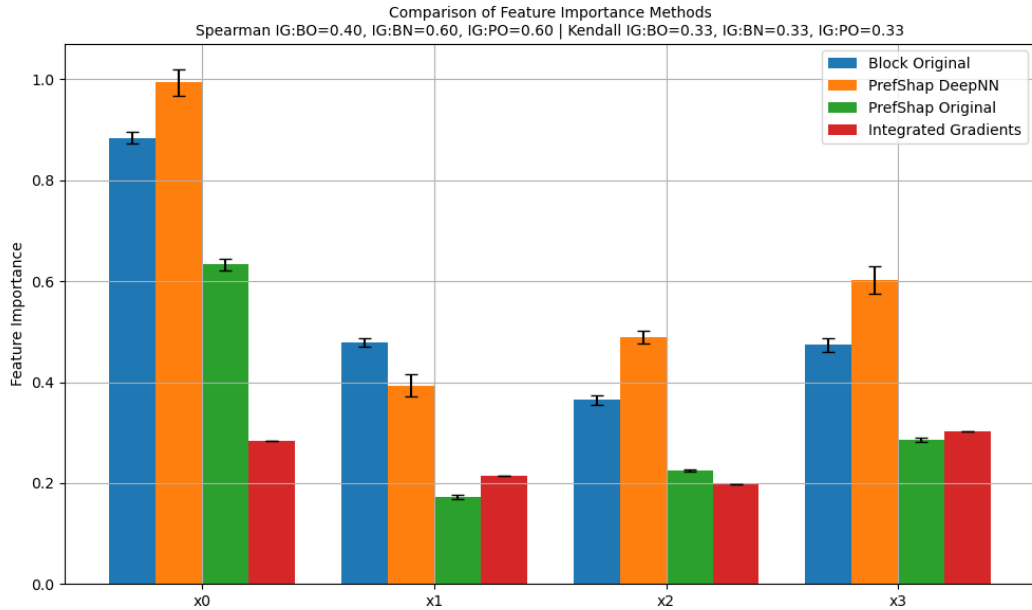


Figure 10: $\sin(x_0), \cos(x_1), \sin(2x_2), \cos(2x_3), \sin(x_0 + x_1), \cos(x_2 - x_3)$

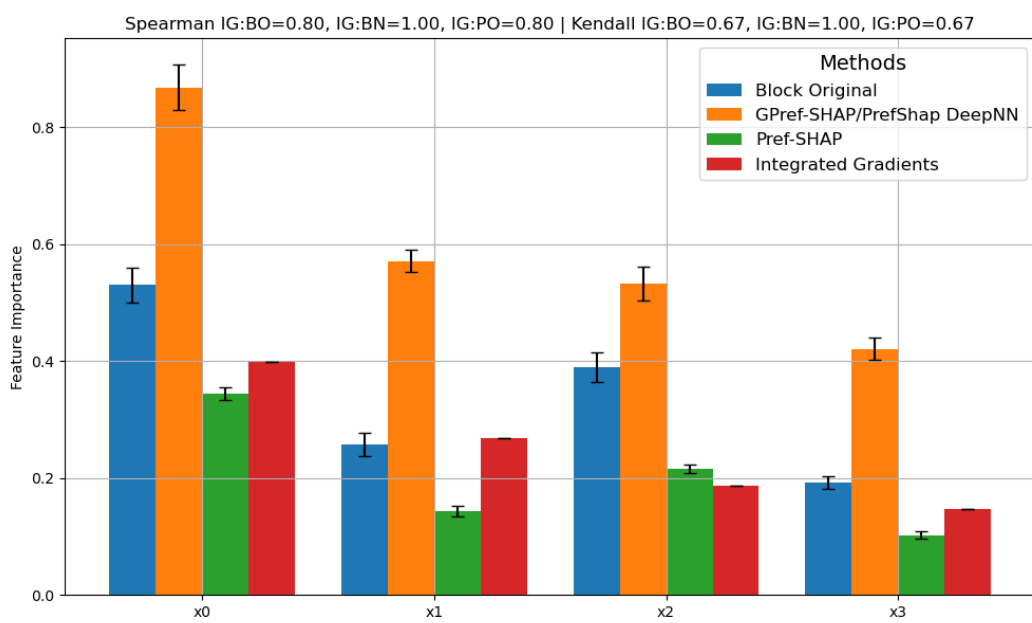


Figure 11: ReLU network(4 input features, 4 mapped features, 8 hidden layers, 16 nodes in each layer)

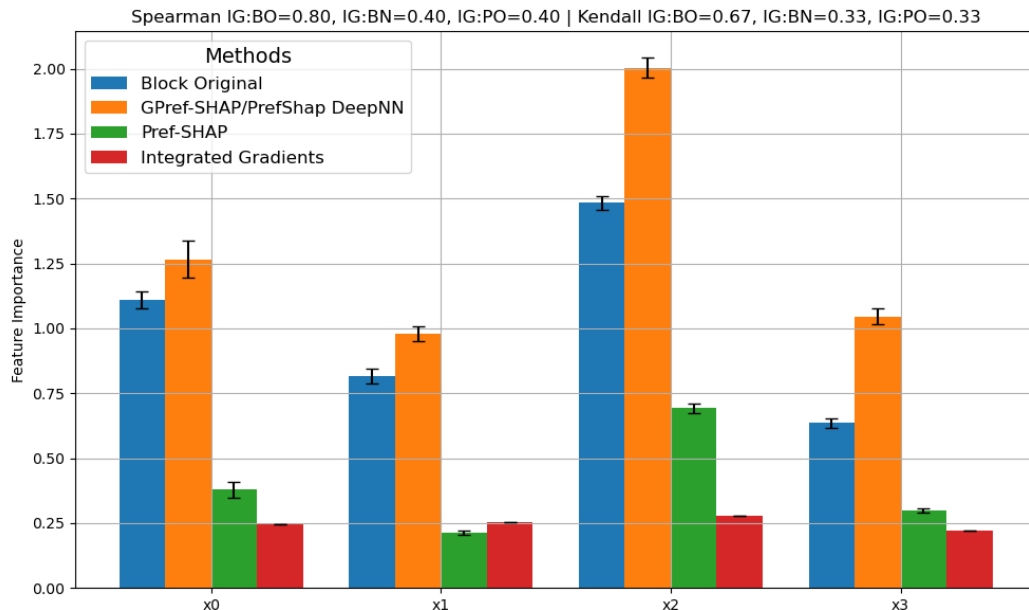


Figure 12: ReLU network(4 input features, 6 mapped features, 8 hidden layers, 8 nodes in each layer)

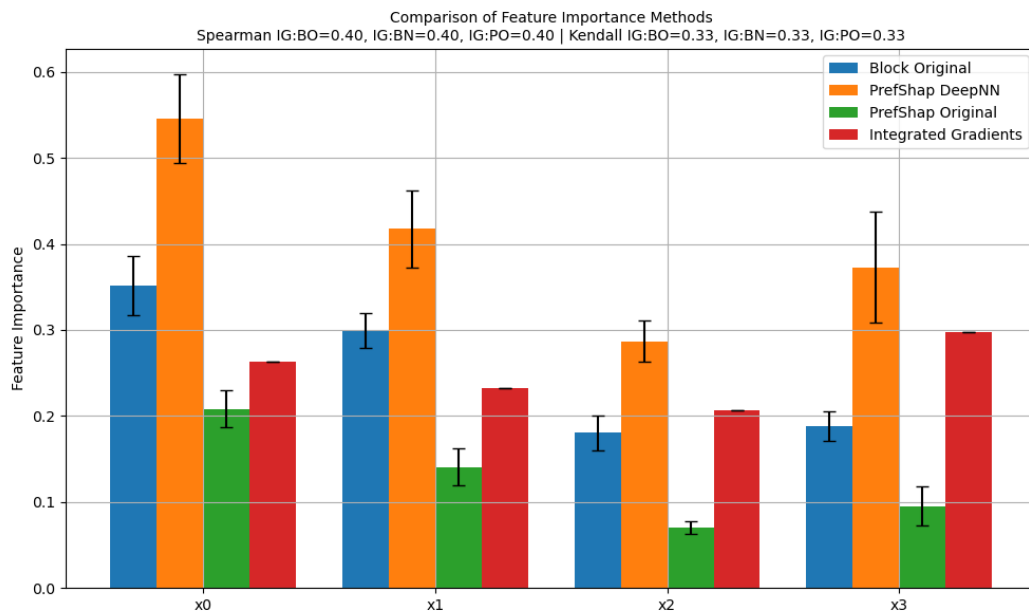
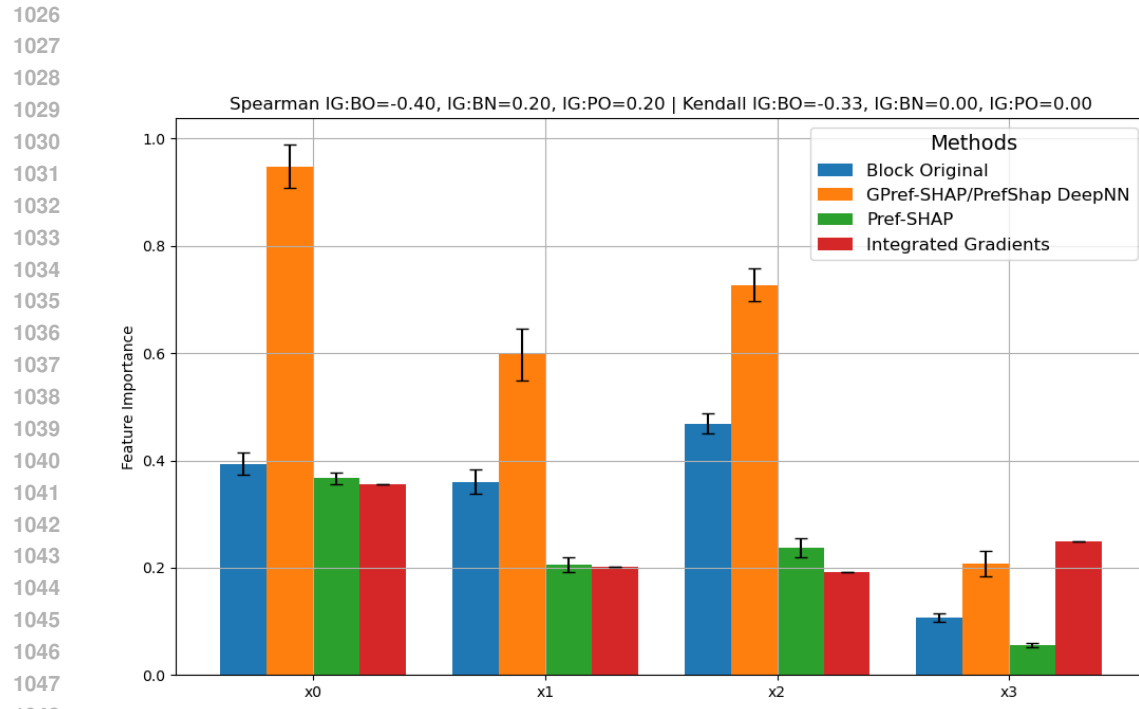


Figure 13: ReLU network(4 input features, 4 mapped features, 16 hidden layers, 16 nodes in each layer)



1049 Figure 14: ReLU network(4 input features, 4 mapped features, 8 hidden layers, 16 nodes in each
1050 layer) for highly correlated data

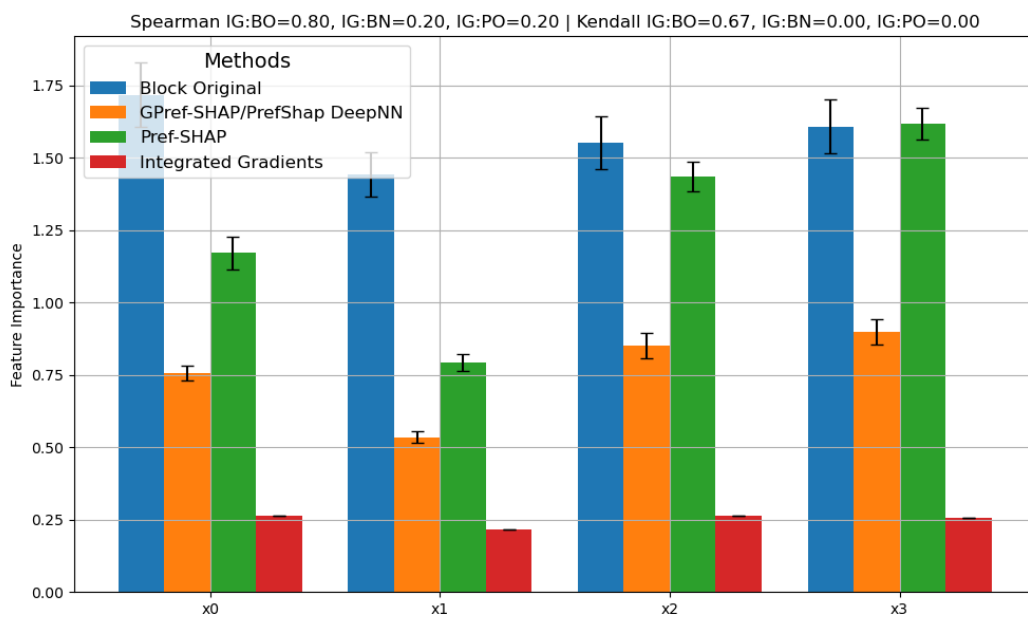
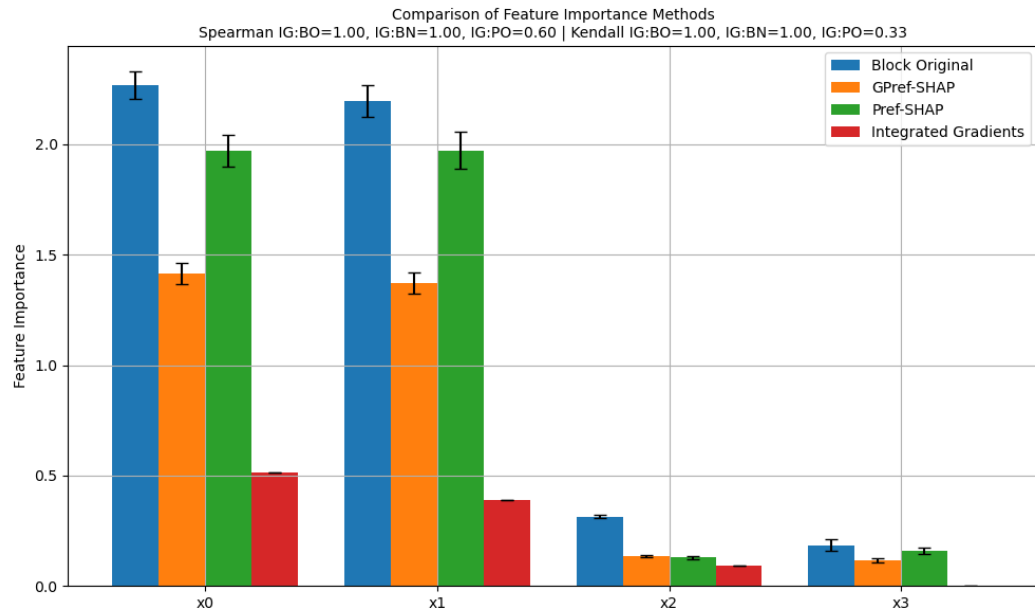
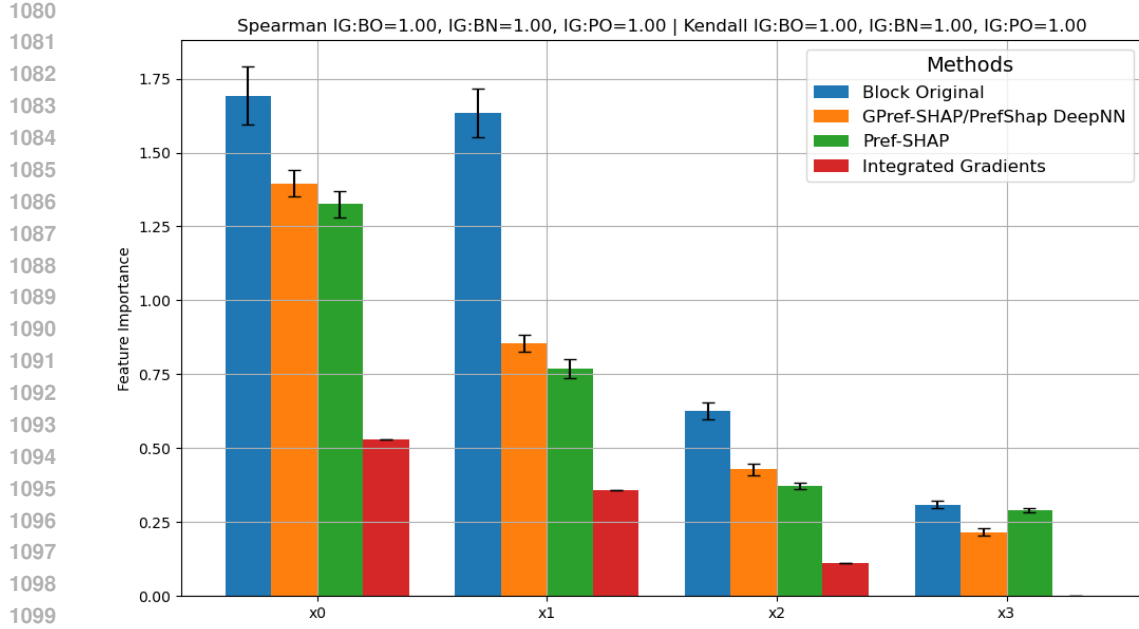


Figure 15: $x_0^2, x_1^2, x_2^2, x_3^2$ for highly correlated data

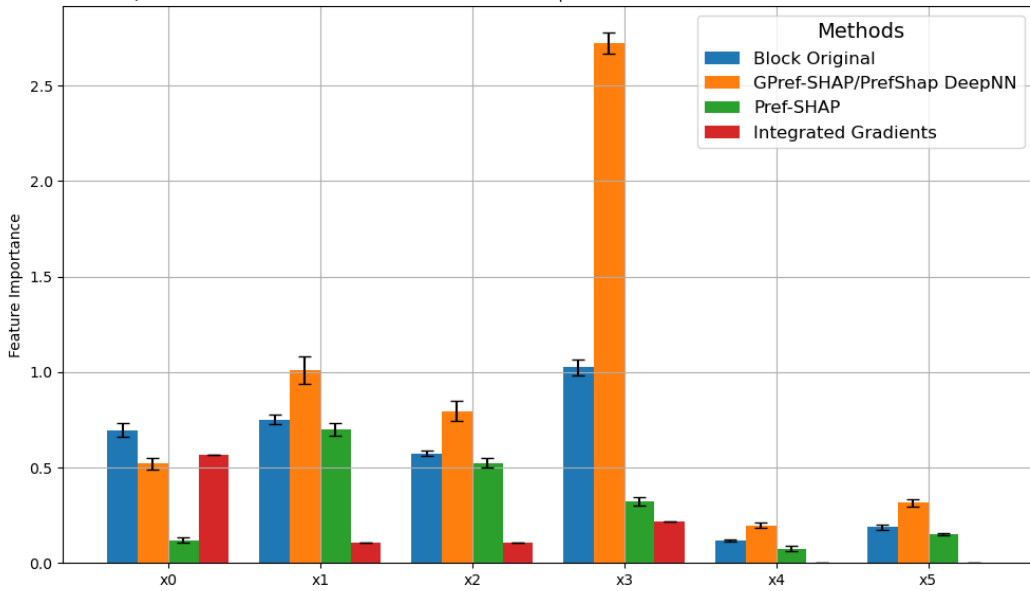


such features in all of them. But in figure 18, Pref-SHAP has more attribution for the dummy feature x_5 than x_0 which is an active feature in the function generation. Also, in figure 17, Pref-SHAP has more feature attribution for x_3 than that of x_2 .

E TEST RMSE AND LINEARITY SCATTER PLOTS FOR THE SYNTHETIC DATA

Figures 21,22,23,24 represent the plots for test RMSE and scatter plots for the synthetic datasets.

1134
1135
1136
1137 Spearman IG:BO=0.77, IG:BN=0.60, IG:PO=0.14 | Kendall IG:BO=0.60, IG:BN=0.47, IG:PO=0.07
1138
1139
1140
1141
1142
1143
1144
1145
1146
1147
1148
1149
1150
1151
1152
1153
1154
1155
1156

Figure 18: $x_0^2, x_1 x_2, \sin(x_3), \cos(x_0)$ with 2 inactive input features

1157
1158
1159
1160
1161
1162
1163
1164 Spearman IG:BO=0.77, IG:BN=0.77, IG:PO=0.60 | Kendall IG:BO=0.60, IG:BN=0.60, IG:PO=0.47
1165
1166
1167
1168
1169
1170
1171
1172
1173
1174
1175
1176
1177
1178
1179
1180
1181
1182
1183
1184
1185
1186
1187

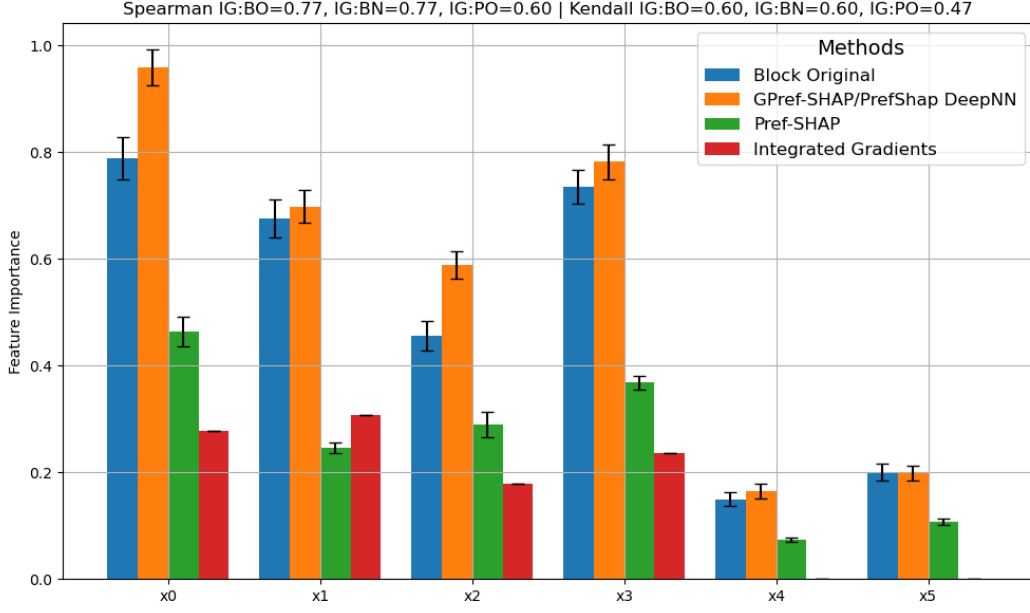


Figure 19: ReLU network(4 active + 2 inactive input features, 6 mapped features, 4 hidden layers, 16 nodes in each layer)

1188

1189

1190

1191

1192

1193

1194

1195

1196

1197

1198

1199

1200

1201

1202

1203

1204

1205

1206

1207

1208

1209

1210

1211

1212

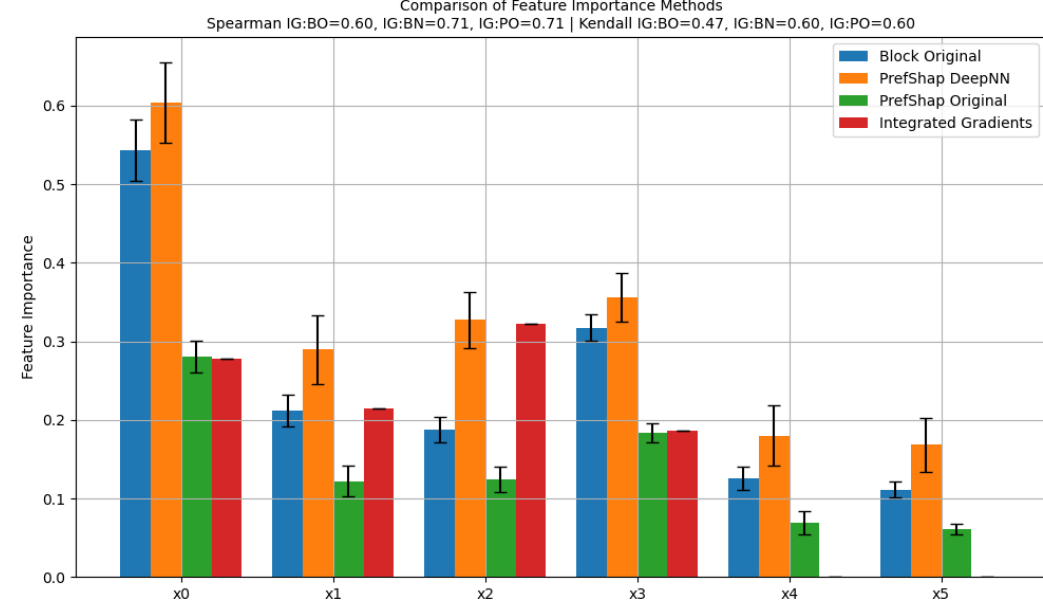


Figure 20: ReLU network(4 active + 2 inactive input features, 4 mapped features, 16 hidden layers, 16 nodes in each layer)

1214

1215

1216

1217

1218

1219

1220

1221

1222

1223

1224

1225

1226

1227

1228

1229

1230

1231

1232

1233

1234

1235

1236

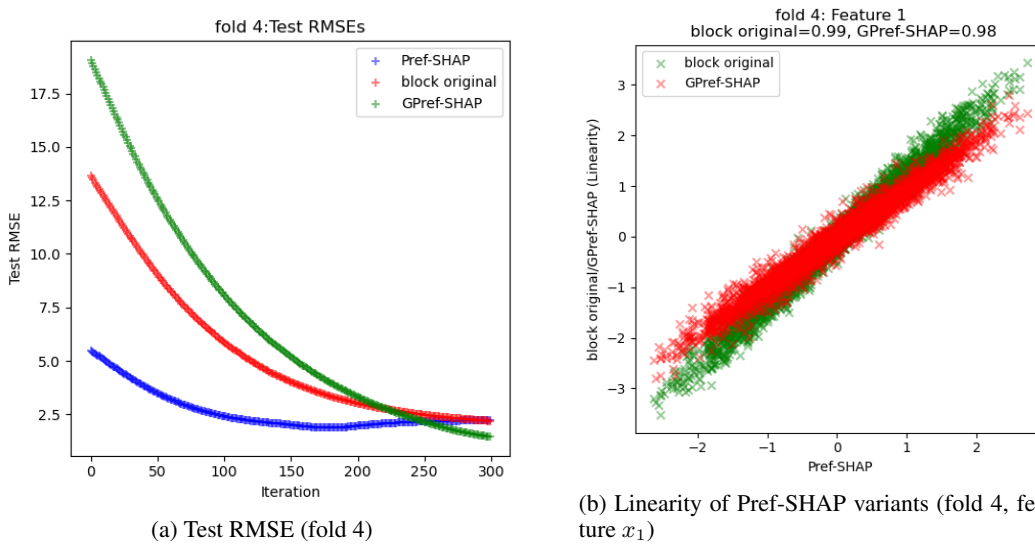
1237

1238

1239

1240

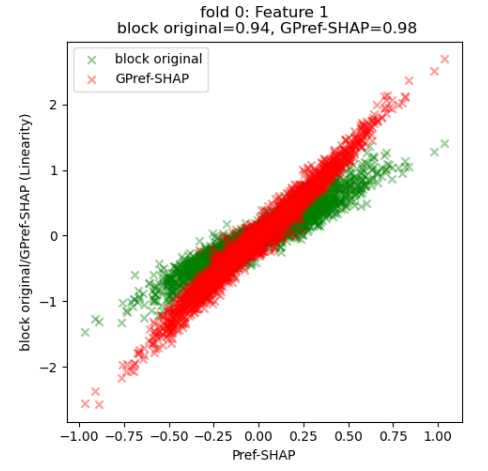
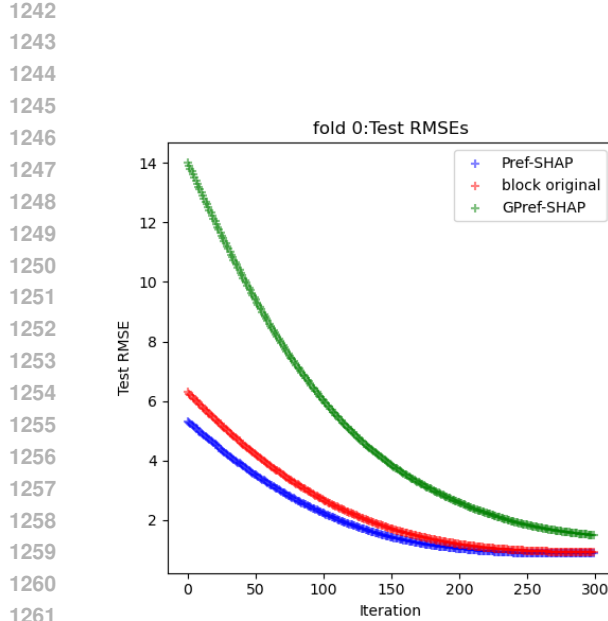
1241



(a) Test RMSE (fold 4)

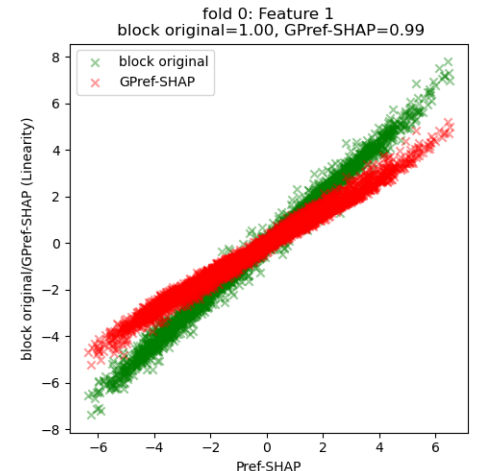
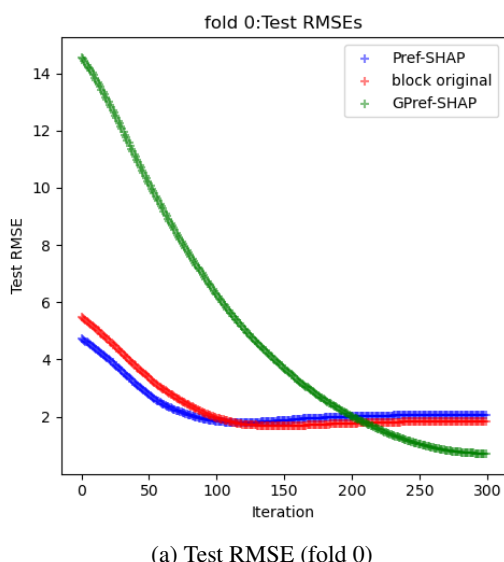
(b) Linearity of Pref-ShAP variants (fold 4, feature x_1)

Figure 21: $x_0^2, x_1 x_2, \sin(x_3), \cos(x_0), \sin(x_1 + x_2), x_3^2$



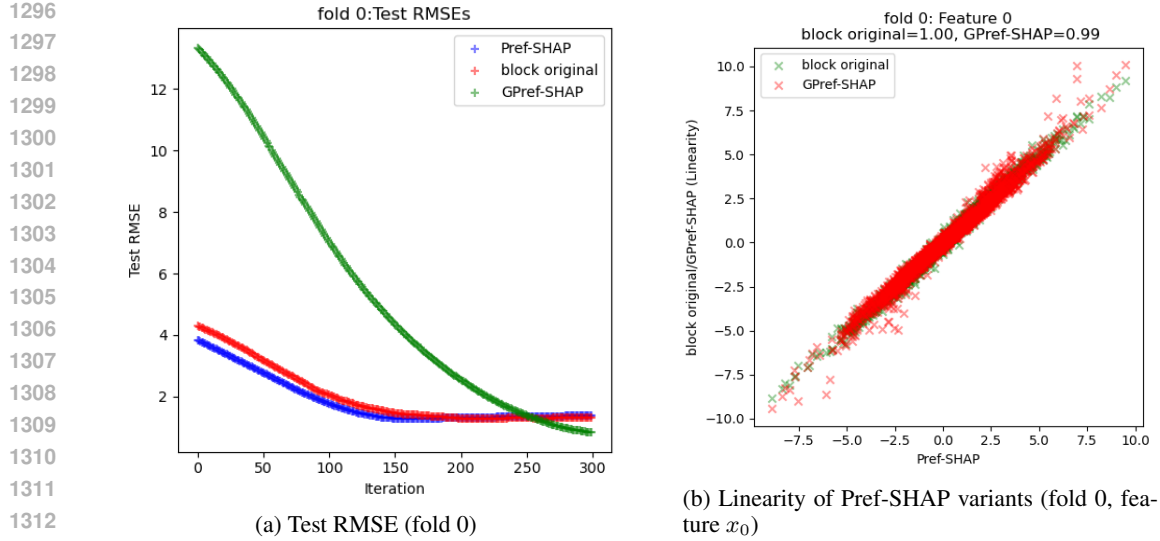
(b) Linearity of Pref-SHAP variants (fold 0, feature x_1)

Figure 22: ReLU network(4 input features, 4 mapped features, 8 hidden layers, 16 nodes in each layer) with highly correlated features



(b) Linearity of Pref-SHAP variants (fold 0, feature x_1)

Figure 23: $x_0^2, x_1^2, x_0x_1, x_0x_2$ with independent features

Figure 24: $x_0^2, x_1^2, x_0x_1, x_0x_2$ with highly correlated features

F USE OF LLMs:

Chatgpt has been used to polish the writing of certain parts in the paper.